

Exploring medium properties using jet substructure measurements in pp and Pb–Pb collisions with ALICE

Hannah Bossi for the ALICE Collaboration^{1,2,*}

¹Yale Wright Laboratory, 272 Whitney Ave, New Haven, CT 06511

²Massachusetts Institute of Technology Laboratory for Nuclear Science 77 Massachusetts Avenue, 26-505 Cambridge, MA 02139-4307

Abstract. Various studies of jet substructure in heavy-ion collisions offer a consistent picture of QCD medium interactions and a diverse path towards further differentiating energy loss mechanisms. Some results, however, remain disjoint: the jet mass and jet angularities, including girth and thrust, are strongly-correlated observables which have given seemingly conflicting answers on the angular quenching of jets traversing the quark–gluon plasma (QGP). ALICE has carried out new systematic measurements of these and other perturbatively-calculable angularities using consistent definitions, resolving the girth-mass problem, and revealing quenching effects at broad angles. Concurrently, applying Soft Drop grooming isolates the narrowing in the core of quenched jets. Grooming can also be employed to resolve medium scattering centers, with varying methods used to focus on regions of the splitting phase space. We present the first application of dynamical grooming in heavy-ion collisions to search for excess $k_{T,g}$ emissions as a signature of point-like scatters, providing new constraints on searches for in-medium Molière scattering. We also present a novel shift from studying jet-medium opacity from the angular perspective to a time-like one. By employing a new time reclustering strategy, we potentially enable a time-dependent study of jet substructure observables. We compare all results to assorted jet quenching models, providing new critical information on medium evolution as a function of angular, momentum, and time structure.

1 Introduction

In hadronic collisions at high energy, partons within the colliding objects can occasionally scatter off one another with a large momentum transfer. The hard-scattered partons then fragment via a parton shower and hadronize into a narrow cone of particles called a jet. The resulting jet and its substructure are ideal internally-generated probes of the physics from the hard scattering scale to the hadronization scale. These proceedings will focus on measurements of jet substructure. In pp collisions where parton fragmentation occurs in vacuum, measurements of the jet substructure are useful for studying both perturbative and non-perturbative quantum chromodynamics (herein referred to as pQCD and npQCD, respectively) as well as the transition between these two regimes. In addition, vacuum jet substructure can also be used to study processes of a specific origin such as quark- vs. gluon-initiated jets. The substructure of jets in heavy-ion collisions is modified due to the presence of the quark–gluon

*e-mail: hannah.bossi@cern.ch

plasma (QGP) formed in these collisions. As a result, jet substructure measurements are uniquely sensitive to the transport and microscopic properties of the QGP. In these proceedings, two different types of jet substructure measurements with the ALICE detector will be discussed. The first (discussed in Sec.2) are jet splittings, which focus on the hard (or parton-level) substructure of the jet. The second category (discussed in Sec. 3) are jet shapes that focus on the distribution of radiation within the jet or its hadron-level substructure.

2 Jet Splittings

Jet splittings refer to hard splittings within the jet that can be identified by reconstructing the jet’s declustering history. These splittings are characterized by a number of variables. For example, the asymmetry of the splitting is characterized by the shared momentum fraction $z \equiv \frac{p_{T,2}}{p_{T,\text{jet}}}$, where $p_{T,2}$ is the p_T of the subleading subjet. The angular scale of the splitting is characterized by $\theta \equiv \frac{\Delta R}{R}$ where ΔR is the angular separation between subjets and R is the jet resolution parameter. The “hardness” of the splitting is characterized by $k_T \equiv p_{T,2} \sin(\Delta R)$. The formation time of the splitting is characterized by τ , as defined in Eq. 1.

$$\tau \approx \frac{p_{T,1} + p_{T,2}}{p_{T,1} p_{T,2} (\Delta R)^2} \quad (1)$$

Often, measurements of jet splittings are coupled with grooming methods that can help isolate the hard splittings within the jet. The measurements discussed in these proceedings employ two different grooming methods; Soft Drop (SD) Grooming [1] and Dynamical Grooming (DyG) [2]. In SD grooming, hard splittings are selected by a cutoff in z where $z > z_{\text{cut}}(\Delta R/R)^\beta$. In the case of DyG this cutoff is generated on a jet-by-jet basis, where the free parameter a is used to specify different hardness metrics for splittings in the declustering sequence as $\kappa^{(a)} = \frac{1}{p_T} \max_{i \in \text{seq.}} z_i (1 - z_i) p_{T,i} (\frac{\Delta R_i}{R})^a$.

Jet substructure techniques can be used in order to search for point-like or “Moliere” scatterings with QGP quasi-particles. These scatterings may lead to an enhancement of large k_T splittings in Pb–Pb collisions relative to pp collisions. However, such measurements are of course also sensitive to the modification of the jet substructure as seen in the groomed shared momentum fraction (z_g) and the groomed ΔR (R_g) distributions [3, 4]. In this approach, one can also utilize various grooming methods to isolate the hard splittings within the jet. The measurement discussed in these proceedings utilizes a DyG procedure with $a = 0.5, 1.0, 2.0$ as well as a SD procedure with $z_{\text{cut}} = 0.2$. The groomed k_T ($k_{T,g}$) distributions for the SD and DyG grooming methods in pp collisions, as well as their ratio to the case of DyG procedure with $a = 0.5$ are shown in the left panel of Fig. 1. Here, there are some noticeable deviations between various methods at lower values of $k_{T,g}$ while at higher values of $k_{T,g}$ the various grooming methods converge. In the right panel of Fig. 1 these distributions are shown in pp and Pb–Pb collisions as well as their ratio in the bottom panel. The ratios reveal a suppression at high $k_{T,g}$ that is in contrast to the enhancement expected for a clear Moliere-like signal, and instead is consistent with the narrowing seen in other angular-dependent substructure observables [3]. The measurements are compared to model calculations of the Hybrid model including the wake, both with and without Moliere effects [5], as well as JETSCAPE v3.5 A22 [6]. The data is well described by the Hybrid model w/o Moliere effects as well as JETSCAPE which includes Moliere effects.

Jet substructure measurements can also be used to probe the temporal structure of the jet through variables such as τ (as defined in Eq. 1) that encode information about pQCD, npQCD, and the transition region. In these proceedings the temporal structure of the jet is only studied in pp collisions, though future studies of Pb–Pb collisions would be useful to

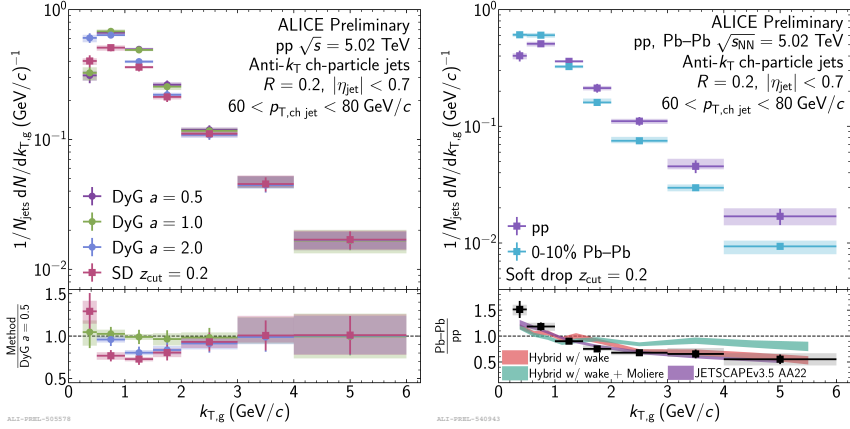


Figure 1. (Left) Groomed k_T distribution for $R = 0.2$ jets from $60 < p_T < 80$ GeV/c in pp collisions for various grooming methods. The ratio to DyG with $a = 0.5$ is shown in the bottom panel. (Right) Groomed k_T distributions in pp and Pb–Pb collisions, with the ratio and model comparisons shown in the bottom panel.

study the time-structure of jet quenching effects [7]. In addition to studying the temporal structure of the jet with τ , one can also perform a τ -based reclustering of the jet by setting $p = 0.5$ in sequential recombination algorithms [8] such that the distance metric converges to $d_{ij} = \min(p_{T,i}^{2p}, p_{T,j}^{2p}) \frac{\Delta R_{ij}^2}{R^2} \sim p_T \theta^2 \sim \frac{1}{\tau}$. This τ -based reclustering scheme is compared for the R_g distribution to the standard C/A scheme [8], which is purely angular-ordered, in the left panel of Fig. 2. In the ratio of these distributions, one can see hints that the τ reclustering scheme selects wider splittings in R_g , assuming angular-ordering in a vacuum shower. Other substructure variables, such as z_g do not appear to have the same degree of sensitivity to the reclustering scheme. The ratio of the distributions shows good agreement with both PYTHIA [9] and HERWIG [10], though there are some deviations in the individual distributions themselves, particularly in the peak of the R_g distribution. In the right panel of Fig. 2 the first measurement of the τ_g distribution at the LHC is presented for both C/A and τ reclustering schemes. Here, there are also some hints that the τ reclustering finds earlier splittings. Additionally, both the distributions themselves as well as their ratios are well described by both PYTHIA and HERWIG.

3 Jet Shapes

Generalized angularities represent a full phase space of observables that probe the p_T and angular dependence of the distribution of radiation with relative weightings κ and α as defined $\lambda_\alpha^\kappa \equiv \left(\frac{p_{T,i}}{p_{T,jet}}\right)^\kappa \left(\frac{\Delta R_{i,jet}}{R}\right)^\alpha$ [11]. ALICE has performed a measurement of these angularities both in pp [12] and Pb–Pb collisions such that the modification of these distributions in response to the QGP can be measured. These distributions are also compared to models, with generally good agreement. From these measurements, one can see that the core of the jet is more modified than the large-angle distribution. This is additionally reinforced by the fact that, when comparing the groomed to the ungroomed jet mass distributions, the groomed distributions show a much larger degree of modification. These measurements also showed that utilizing a pp reference effectively addresses the girth-mass puzzle where in Run 1 results the girth and the mass showed different degrees of modification.

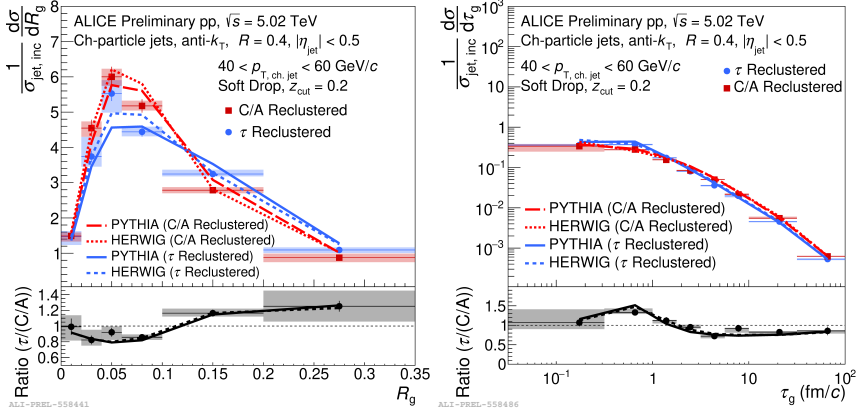


Figure 2. R_g (Left) and τ_g (Right) distributions for $R = 0.4$ jets with $40 < p_{T,\text{ch,jet}} < 60$ GeV/c in pp collisions with a SD grooming procedure with a $z_{\text{cut}} = 0.2$ reclustering with both the C/A reclustering scheme as well as the τ reclustering scheme. Comparisons to PYTHIA and HERWIG are also shown and the ratio between the distributions with these two reclustering schemes is shown.

4 Conclusions

Overall, measurements of jet substructure are uniquely sensitive probes of different QCD scales and their modification in the QGP. ALICE continues to make significant progress in understanding jet substructure in vacuum and in the QGP. In these proceedings, measurements of the $k_{T,g}$ and the τ_g distributions in pp collisions provide a precision test of QCD while also providing comparisons between grooming methods and reclustering techniques. The measurements in Pb–Pb collisions, where a QGP is formed, discussed in these proceedings, the generalized angularities and the k_T distributions, both show a general narrowing trend with no clear Moliere signal. Both of these measurements are key for tests of jet-medium interactions. To further the use of these jet substructure measurements, new techniques to help extend the precision and kinematic reach of the measurements are needed. These will be especially useful in analyzing the wealth of new data collected during Run 3 of the LHC.

References

- [1] A.J. Larkoski, S. Marzani, G. Soyez, J. Thaler, JHEP **05**, 146 (2014)
- [2] Y. Mehtar-Tani, A. Soto-Ontoso, K. Tywoniuk, Phys. Rev. D **101**, 034004 (2020)
- [3] S. Acharya et al. (ALICE Collaboration), Phys. Rev. Lett. **128**, 102001 (2022)
- [4] Y.T. Chien, I. Vitev, Phys. Rev. Lett. **119**, 112301 (2017), 1608.07283
- [5] Z. Hulcher, D. Pablos, K. Rajagopal, Acta Phys. Polon. Supp. **16**, 1 (2023)
- [6] Y. Tachibana et al. (JETSCAPE) (2023), arXiv:2301.02485
- [7] L. Apolinário, A. Cordeiro, K. Zapp, Eur. Phys. J. C **81**, 561 (2021)
- [8] M. Cacciari, G.P. Salam, G. Soyez, JHEP **04**, 063 (2008)
- [9] C. Bierlich et al. (2022), arXiv:2203.11601
- [10] J. Bellm et al., Eur. Phys. J. C **80**, 452 (2020)
- [11] A.J. Larkoski, J. Thaler, W.J. Waalewijn, JHEP **11**, 129 (2014)
- [12] S. Acharya et al. (ALICE Collaboration), JHEP **05**, 061 (2022)